diversity

MDPI

Article

Floral Trait and Mycorrhizal Similarity between an Endangered Orchid and Its Natural Hybrid

Jacopo Calevo [1,2,3,*], Miriam Bazzicalupo [4], Martino Adamo [1], Francesco Saverio Robustelli della Cuna [5], Samuele Voyron [1,6], Mariangela Girlanda [1,6], Karl J. Duffy [2], Annalisa Giovannini [7] and Laura Cornara [4]

1 Department of Life Sciences and Systems Biology (DBIOS), University of Torino, 10125 Torino, Italy; martino.adamo@unito.it (M.A.); samuele.voyron@unito.it (S.V.); mariangela.girlanda@unito.it (M.G.)
2 Department of Biology, University of Naples Federico II, Via Cinthia, 80126 Naples, Italy; karljoseph.duffy@unina.it
3 School of Molecular and Life Sciences, Curtin University, Perth, WA 6102, Australia
4 Department of Earth, Environment and Life Sciences (DISTAV), University of Genova, 16132 Genova, Italy; miriam.bazzicalupo@gmail.com (M.B.); laura.cornara@unige.it (L.C.)
5 DDS—Department of Drug Sciences, University of Pavia, 27100 Pavia, Italy; fsaveriorobustelli@unipv.it
6 Istituto per la Protezione Sostenibile delle Piante, UOS Turin (CNR-IPSP), Viale Mattioli, 25, 10125 Turin, Italy
7 Centro di ricerca Orticoltura e Florovivaismo (CREA-OF), Corso degli Inglesi 508, 18038 Sanremo, Italy; annalisa.giovannini@crea.gov.it
* Correspondence: jacopo.calevo@unina.it

Abstract: Hybridization can often lead to the formation of novel taxa which can have traits that resemble either or both parental species. Determining the similarity of hybrid traits to parental taxa is particularly important in plant conservation, as hybrids that form between rare and common taxa may more closely resemble a rare parental species, thereby putting the rare parental taxon at further risk of extinction via increased backcrossing and introgression. We investigated the floral (morphological and chemical) traits and orchid mycorrhizal (OrM) fungal associations of the endangered orchid *Orchis patens*, its more common sister species *O. provincialis*, and their natural hybrid *O.* × *fallax* in natural sympatric populations. We found that both morphological and chemical floral traits of *O.* × *fallax* are shared by the parents but are more similar to *O. patens* than *O. provincialis*. OrM fungi were shared among all three taxa, indicating that the availability of OrM fungi should not represent a barrier to establishment of individuals of any of these taxa. These results suggest that *O.* × *fallax* may be able to expand its distribution within a similar niche to *O. patens*. This highlights the importance of quantifying differences between hybrids and parental taxon in species conservation planning.

Keywords: Orchidaceae; essential oils; mycorrhizal fungi; hybridization; floral morphology; osmophores; conservation

Citation: Calevo, J.; Bazzicalupo, M.; Adamo, M.; Robustelli della Cuna, F.S.; Voyron, S.; Girlanda, M.; Duffy, K.J.; Giovannini, A.; Cornara, L. Floral Trait and Mycorrhizal Similarity between an Endangered Orchid and Its Natural Hybrid. *Diversity* **2021**, *13*, 550. https://doi.org/10.3390/d13110550

Academic Editor: Federico Sebastiani

Received: 7 October 2021
Accepted: 28 October 2021
Published: 30 October 2021

1. Introduction

Hybridization among plant species is common in the wild and is thought to be a driving force in evolution [1,2]. Indeed, plant speciation through hybridization (such as allopolyploidy or homoploid hybrid speciation) is widespread in the plant kingdom [3–5]. However, hybridization can also lead to introgression and the loss of unique genetic identities within populations [6,7]. This is particularly true when rare species co-occur and hybridize with more common and widespread related taxa [8,9]. In these cases, hybridization may drive extinction of rarer taxa [10–12]. The maintenance of species boundaries depends on reproductive barriers to isolate sexually compatible species which grow sympatrically [13,14]. These barriers can be divided in pre-zygotic, which prevent individuals of different species from mating (e.g., by emitting different scents that attract different pollinators, different flowering phenology, habitat separation or geographic distribution) and post-zygotic barriers, such as hybrid sterility, fruit abortion, production

of non-viable seeds or, in the case of plants that depend on fungi to recruit from seed, limitation of suitable mycorrhizas [15,16].

Hybridization is particularly common in the Orchidaceae, a plant family renowned for its diverse pollination strategies and floral traits [17]. However, in regions such as the Mediterranean, orchid pollination is almost never specialized [4]. As a result, high levels of natural hybridization have been documented among orchid species [18]. This is particularly common in spring-flowering food deceptive orchids, as these orchids flower early to deceive naïve insects as they do not provide a nectar or pollen reward to insect pollinators, instead relying on floral visual, and perhaps olfactory, cues to attract insect pollinators. Therefore, increased similarity in floral traits between two species may increase the probability of hybridization. Likewise, increased similarity between a hybrid taxon and one of its parental species may increase the likelihood of backcrossing and potential introgression. Experimental approaches have demonstrated that post-mating barriers (such as fruit set, seed viability, and/or hybrid sterility) are particularly strong in closely related orchid species [19–21]. However, high levels of hybridization are reported in the food-deceptive genera *Anacamptis* and *Orchis* [12,22–24]. This indicates that pre- and/or post-mating barriers are less effective between species within these groups and that hybridization may be a common mechanism in their evolution. Indeed, most of these species are pollinated by generalist insects such as bees, beetles, and flies [22,25,26]. However, a strong post-mating pre-zygotic isolation may also have evolved in these species as a consequence of chromosomal differences [27,28]. Post-zygotic barriers, for example, are expected to ensure reproductive isolation in populations with various ploidy levels [13], but the possibility of gene flow across taxa with various ploidies has long been acknowledged (though it is uncommon) [29,30].

Since mycorrhizal fungi (OrM) are necessary for orchid seed germination, development, and subsequent seedling establishment [31,32], it has been hypothesized that OrM fungal availability may act as a post-mating barrier in sympatric populations [20]. A study in hybrid *Caladenia* species from Australia showed that OrM fungi isolated from parental taxa can induce germination of hybrid seeds but also that hybrid can associate with genetically different OrM fungi [33]. Recent studies demonstrated that OrM fungi are usually shared among closely related orchid species that occur in the same population [34–36]. However, it has been suggested that polyploidy, which is recognised as a mechanism of sympatric speciation, can induce a shift in mycorrhizal association in plants growing sympatrically [37].

Here, we investigate two pre-zygotic traits, floral micromorphology and floral chemical composition, and one important post-zygotic factor in the establishment of new orchid individuals, OrM fungi. For this, we sampled a hybrid zone between two food-deceptive Mediterranean *Orchis* species with different ploidy levels, the Endangered tetraploid *O. patens* [38,39] and the widespread diploid *O. provincialis*, and their natural triploid hybrid *O.* × *fallax* [39], whose number of individuals is rapidly increasing (personal observation) in two populations in Northwest Italy. Specifically, we tested the hypothesis that there are differences between the two parental taxa in both their floral and OrM fungal associations but that their hybrid taxon is intermediate in both its floral traits and shares fungi with both parental species.

2. Materials and Methods

2.1. Plant Material

Flowers of *Orchis patens* (Figure 1a), *O.* × *fallax* (which was determined based on morphology; Figure 1b) and *O. provincialis* (Figure 1c) have been sampled from two populations, Breccanecca (44.3152° N–9.35614° E 255 m asl) and Pieve Ligure (44.37890° N–9.08749° E 400 m asl; Genova, Italy), where these taxa grow sympatrically. Breccanecca is characterized by olive groves (hosting both rich grasslands vegetation and semi-dry grassland vegetation), and mesophilous broad-leaved mixed woods on hillslopes. Pieve Ligure is

a dry grassland and garrigue habitat and thermophilous Mediterranean woods in which artificial pine forests are also present.

Figure 1. Inflorescences of (**a**) *Orchis patens*, (**b**) *O.* × *fallax*, and (**c**) *O. provincialis*.

Five inflorescences were collected from individuals of all three orchid taxa in full anthesis and then processed as described in the following subsections. Due to small population sizes and the high conservation status of *O. patens*, we restricted our root sampling for fungal metabarcoding to four individuals of *O. patens*, and five individuals from *O.* × *fallax* and *O. provincialis* each, collected in the Breccanecca population. Hybrid plants showing typical intermediate characteristics such as long spur and green stem (Figure 1b) were selected since no molecular data to confirm the possibility of backcrossing with one or both parental species is currently available. Plant material was sampled with the permission of Regione Liguria (D.G.R. n. 362- 29/01/2018)

2.2. Morphological Analysis

Light and Scanning Electron Microscopy

Four fresh flowers of *O. patens*, *O.* × *fallax*, and *O. provincialis* were examined using light microscopy (LM), and another four flowers were processed for scanning electron microscopy (SEM) analyses.

Untreated epidermal peels were observed by both transmitted light and epifluorescence using a Leica DM2000 Microscope coupled to a computer-driven DFC 320 camera (Leica Microsystems, Wetzlar, Germany). To detect the presence and autofluorescence of secondary metabolites, samples were examined under a UV filter (340–380 nm) according to Talamond et al. [40]. In addition, fresh tissues were stained with Sudan III to detect total lipids or with 0.001% Neutral Red to verify the presence and to measure secretory activity of the osmophores, structures involved in scent production, as performed by Stern et al. [41].

For SEM analyses, flowers were fixed in the ethanol-based working solution FineFIX (Milestone, Bergamo, Italy), and incubated overnight at 4 °C; fixed samples were then dehydrated through an ascending series of ethanol (70–80–90–100%, 1 h for each passage), following Chieco et al. [42]. Samples were processed with a Critical Point Drier (K850CPD 2M Strumenti S.r.l., Roma, Italy), and mounted on aluminium stubs where they were sputter-coated with a 10 nm gold particle layer. Plant material was finally observed with a VEGA3-Tescan-type LMU microscope (Tescan Orsay Holding, a.s., Brno, Czech Republic), at an accelerating voltage of 20 kV.

Flower parts descriptive terminology was adopted according to Bateman et al. [43] while we followed Akbulut et al. [44] for the description of papillae.

2.3. Analysis of Essential Oils

2.3.1. Isolation of Volatile Fraction

Samples of flowers of *O. patens* (6.15 g), *O. provincialis* (5.56 g), and *O.* × *fallax* (2.91 g) to which octyl octanoate (98%, Sigma-Aldrich, Inc., St. Louis, MI, USA) was added as internal standard, were steam distilled with odour-free water for 3 h. Due to the low yield of essential oil, it is difficult if not impossible to stratify on the aqueous phase obtained from steam distillation. Therefore, solvent extraction is necessary to isolate the essential oil. The distillate was extracted with methylene chloride (3 × 100 mL) (Merck, Darmstadt, Germany), dried over anhydrous sodium sulfate (Sigma-Aldrich, Inc., St. Louis, MI, USA), and concentrated at first with a rotary evaporator and subsequently using a gentle stream of N_2 for successive GC/FID and GC/MS analyses [45].

2.3.2. Fractionation and Alkylthiolation of Alkenes

Each sample was subjected to selective purification process [46] and alkylthiolation reaction [47]. The dimethyl disulfide adducts were identified, and the positions of the methyl sulfide substituents were deduced from the fragmentation pattern.

2.3.3. GC-FID Analysis

The analyses were carried out using a Hewlett Packard model 5980 GC, equipped with Elite-5MS (5% phenyl methyl polysiloxane) capillary column of 30 m × 0.32 mm i.d. and film 0.32 µm thick. It was used as a carrier gas at a flow of 1 mL/min. One µL aliquots of essential oil were manually injected in splitless mode. The oven temperature program included an initial isotherm of 40 °C for 5 min, followed by a temperature ramp to 260 °C at 4 °C/min, and a final isotherm at this temperature for 10 min. Injector and detector temperatures were set at 250 and 280 °C, respectively. The relative amount of each component was calculated based on the corresponding FID peak area without response factor correction. Analyses were performed in triplicate.

2.3.4. GC-MS Analysis

The analyses were carried out using a GC Model 6890 N, coupled to a benchtop MS Agilent 5973 Network, equipped with the same capillary column and following the same chromatographic conditions used for the GC/FID analyses. The carrier gas was He at a constant flow of 1.0 mL/min. The essential oils were diluted before analysis and 1.0 µL was manually injected into the GC system in splitless mode. The ion source temperature was set at 200 °C, while the transfer line was at 300 °C. The acquisition range was 40–500 amu in electron-impact (EI) positive ionization mode using an ionization voltage of 70 eV.

2.3.5. Identification of the Components of the Volatile Fractions

The identification of the volatile oil components was performed by their retention indices (RI) and their mass spectra [48], and by comparison with a NIST database mass spectral library, as well as with data from the available literature [49]. Retention indices were calculated by Elite-5MS capillary columns using an n-alkane series (C_6–C_{35}) (Sigma-Aldrich, Inc., St. Louis, MI, USA) under the same GC conditions as for samples. The relative amount of each component of the oil was expressed as percent peak area relative to total peak area from GC/FID analyses of the whole extracts. The quantitative data were obtained from GC/FID analyses by an internal standard method and assuming an equal response factor for all detected compounds.

2.4. Fungal Metabarcoding from Roots

2.4.1. DNA Extraction and Amplification

To detect potential orchid mycorrhizal (OrM) fungi of the three taxa, we extracted genomic DNA from roots with the DNeasy Plant Mini Kit by Qiagen (Hilden, Germany) following manufacturer's instructions. DNA quantity and quality were assessed by spectrophotometry (ND-1000 Spectrophotometer NanoDrop; Thermo Scientific, Wilmington, Germany).

DNA amplification was performed as described in Calevo et al. [36] by means of a semi-nested PCR. Briefly, the entire ITS region was amplified with the primers ITS1-OFa, ITS1-OFb and ITS4-OF primers (OF), and primers ITS1 and ITS4tul (Tul) specifically designed for OM fungi [50]. The ITS2 region was amplified, from the previously amplified ITS products, with the ITS3mod and ITS4 [51,52] tagged primers. Each sample was amplified in three replicates. PCR products were checked on 1% agarose gel, and replicates were pooled together and purified using the Wizard SV Gel and PCR Clean-Up System (Promega, Madison, WI, USA), following manufacturer's instructions. Purified amplicons were quantified with Qubit 2.0 (Thermo Fisher Scientific, Waltham, MA, USA), by means of the Qubit™ dsDNA BR Assay Kit. Sequencing libraries prepared with equimolar amounts of purified PCR products were paired-end sequenced using the Illumina MiSeq (2 × 250 bp) by IGA Technology Services Srl (Udine, Italy).

2.4.2. Data Analysis and Bioinformatics

Data were analysed as described in Calevo et al. [36]; summarizing, paired-end reads from each library were merged using PEAR v.0.9.2 [53], setting the quality score threshold at 28 and the minimum length of reads after trimming at 200 bp. The assembled reads were then processed with the Quantitative Insights into Microbial Ecology (QIIME) v.1.8 software package [54]. Operational Taxonomic Units (OTUs) were defined with an open reference-based clustering strategy, by means of the USEARCH61 method [55], at 98% similarity; OTUs encompassing less than 10 sequences were removed [52]. Taxonomy assignment and OTU picking were performed by using the full "UNITE + INSD"; dataset database version 7.2 for QIIME as a reference [56,57]; the BLAST algorithm [58] was used for taxonomy assignment as described in Calevo et al. [36]. The OMF OTU representative sequences were submitted to GenBank and registered under the following string of accession numbers: OK335158-OK335175.

Further analyses were focused on tulasnelloid, ceratobasidioid, serendipitoid, and sebacinoid fungi, which are common OrM symbionts in the genus *Orchis* [34,36]. Their OTU representative sequences were used to create a phylogeny with a maximum likelihood (ML) approach. Sequences were aligned using the program MUSCLE [59] with default conditions for gap opening and gap extension penalty in MEGA v.7.0.26 [60]. ML estimation was performed with RAxML v.8 [61] through 1000 bootstrap replicates [62] using the GTR + GAMMA algorithm on CIPRES Science Gataway [63]. Bootstrap values were mapped on the best tree using the –f option of RAxML and -x 12345 as a random seed. Nodes with a bootstrap value $\geq$70% were considered as well supported.

All further analyses were performed with R v4.1.1 [64] and R studio v1.4.1103 [65]. OTU table was rarefied to 2359 reads in order to make samples comparable with the rrarefy function from the 'vegan' R package v2.5-7. We calculated OTU frequency as: (number of reads per plant taxa)/(total number of reads), and then we plotted the OTUs on a ternary plot using 'ggtern' v3.3.5 R package [66]. Ternary plots (similarly to Venn-diagrams) assign elements to one or more sets, considering their relative frequency. We used a random forest [67] approach to classify plant taxa basing on their mycorrhizal community, this approach is useful to understand the most influencing (the relative importance being calculated as mean decrease Gini score) OTUs shaping a microbial community. We classified orchids mycorrhizal communities using the randomForest function with the 'randomForest' v4.6-14 R package [68] with a Breiman's algorithm. We used orchid taxa as variables and rarefied OTU table as matrix of predictors.

3. Results

3.1. Microscopy

The longitudinal section of the spurs revealed that the inner surface of *Orchis patens* and *O.* × *fallax* were covered with papillae having different length (Figure 2a,b), while *O. provincialis* presented more or less protuberant epidermal cells as already stated by Bell et al. [69] (Figure 2c,i). In *O. patens*, two epidermal protuberances were also observed: one near the spur entrance and another one with elongated papillae positioned near the spur apex (Figure 2a, arrows). A similar papillose protuberance, although less swollen, has been observed also near the spur apex of *O.* × *fallax* (Figure 2b, arrow). No internal extroverted structures have been found in the spur of *O. provincialis* (Figure 2c).

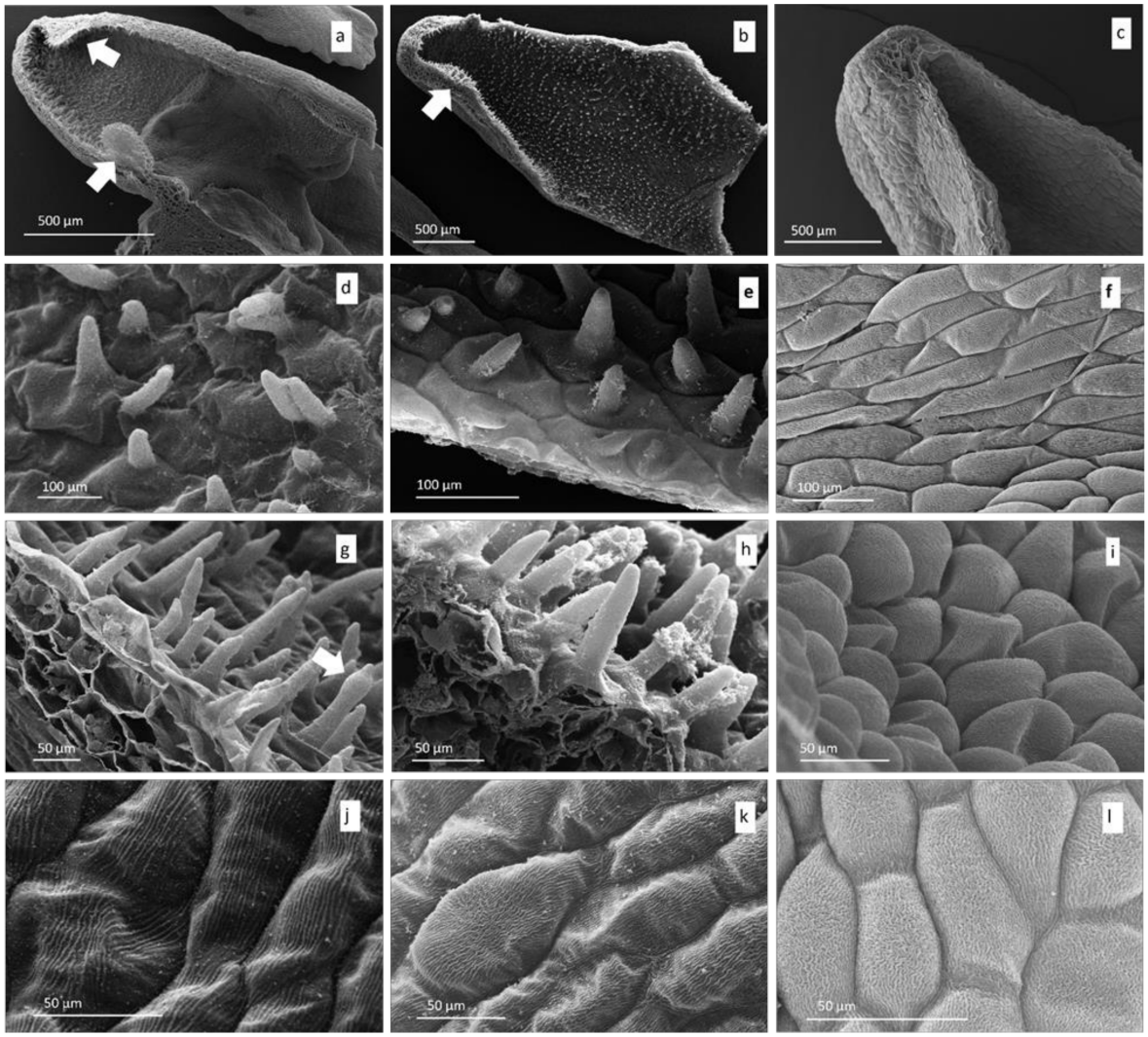

Figure 2. SEM micrographs of the spur of *Orchis patens*, *O.* × *fallax*, and *O. provincialis*. (**a**) *O. patens*: longitudinal section of the spur showing papillae which gradually increase in length. Two internal protuberances are indicated by the arrows; (**b**) *O.* × *fallax*, spur in longitudinal section: papillae gradually increase in length while moving towards the spur apex, where an internal papillose protuberance is present (arrow); (**c**) *O. provincialis*, apical portion of the spur; (**d**) conical papillae from the spur entrance of *O. patens*; (**e**) *O.* × *fallax*, spur entrance: conical papillae are covered with secreted material; (**f**) *O. provincialis*: view of the epidermal cells from the spur entrance; (**g**) *O. patens*: elongated papillae from the median/apical portion. Arrow indicates one of the uniseriate trichomes recorded inside the spur; (**h**) elongated papillae from the internal surface of the median/apical portion of the spur of *O.* × *fallax*. Abundant secreted material covers the papillae; (**i**) *O. provincialis*, epidermal cells from the apical portion of the spur; (**j**) *O. patens*, spur's external surface: parallel straight ornamentations on epidermal cells; (**k**) *O.* × *fallax:* spur's external surface: cell surfaces with sinuous to vermiform striations; (**l**) *O. provincialis:* cells from the external surface of the spur are densely covered with sinuous-vermiform striations.

In *O. patens*, papillae had an expanded base, were conical in shape, and displayed straight radiated cuticular striations. Near the spur entrance, papillae were medium-sized and more or less pyramidal (Figure 2d). These elements gradually increased in length while approaching to the spur apex, where they were more elongated (Figure 2g); some swollen elements, defined as uniseriate trichomes by Naczk et al. [70], were occasionally present (Figure 2g, arrow). This complex of characters (type of cuticular striations, their morphology, and the increasing size of the papillae along the spur internal surface) has also been observed in *O.* × *fallax* (Figure 2b,e,h). In *O. provincialis*, cells located near the spur entrance were prolate and covered by linear cuticular striations which sometimes turned into vermiform (Figure 2f), while cells at the spur apex were more swollen and rounded/sub-prolate with sinuous vermiform striations (Figure 2i).

Characteristic cuticular ornamentations were also present on cells from the spur external surface. In *O. patens*, cells showed parallel linear striations (Figure 2j). In *O. provincialis*, these were markedly sinuous to vermiform (Figure 2l). In *O.* × *fallax* (Figure 2k) striations were closer together and more sinuous than in *O. patens* but less vermiform than in *O. provincialis*.

In *O. patens* (Figure 3a), the labellum was smaller and narrower than those of *O.* × *fallax* (Figure 3b) and *O. provincialis* (Figure 3c). Labellar surfaces of all the three taxa showed deep median grooves along the central longitudinal axis: in the case of *O. patens* (Figure 3a), the groove was smaller in width with less high margins than the other two orchids (Figure 3b,c). All of the three taxa also had further shallower grooves in labellar arms and torso (Figure 3a–c).

In the groove's centre of *O. patens* and *O.* × *fallax*, papillae were conical to conical-villiform, while in the groove margins they were conical-elongated to villiform (Figure 3d,e). In all of the three taxa, towards the labellum leg portion along the groove margins, papillae gradually decreased their length and changed into elongated/conical to conical. In the torso region of *O. provincialis*, villiform papillae were diffused both in the groove centre and in the margins (Figure 3c,f). In *O. patens*, cells from this region displayed thick linear striations (Figure 3d). These ornamentations were more numerous and more sinuous/vermiform in both *O.* × *fallax* and *O. provincialis* (Figure 3e,f).

In the torso, arms, and legs of the labellum of *O. patens*, papillae were more flattened to slightly conical. Radial linear to vermiform cuticular striations have also been recorded (Figure 3h,k). In *O.* × *fallax*, papillae from these regions were more frequently conical-shaped, sometimes villiform, and showed radial linear to vermiform striations (Figure 3i,l). *Orchis provincialis* showed more often conical to villiform papillae, with the latter ones as the most diffused type in other zones of the labellum's torso (Figure 3c); their cuticular striations were radial linear to vermiform at the papillae tip (Figure 3j,m).

Histochemical features and the presence of cytoplasmatic contents have been recorded by LM. All of the size classes of conical papillae inside the spur of *O. patens* were stained by Neutral Red, indicating osmophoric activity (Figure 4a,e). Under UV excitation, all these structures emitted blue autofluorescent signals (Figure 4b–d). Autofluorescence varied from weak to intense light blue when cytoplasmatic content was present, indicating that polyphenols (occasionally hydroxycinnamic acids) were abundant in the secretion. In addition, a weak affinity to Sudan III was observed (not shown). A similar reaction to all of the treatments has been observed also for the papillae inside the spur of *O.* × *fallax* (Figure 4f–k). However, SEM analyses highlighted that in this taxon papillae from the median-apical region of the spur were significantly covered by exudated organic residues (Figure 4h). In *O. provincialis*, no osmophoric activity has been recorded in spur epidermal cells. Their cytoplasmatic content showed only a weak affinity to Sudan III (Figure 4i). Under UV light, only a weak blue autofluorescent signal coming from the lignified cell walls has been detected (Figure 4m,n).

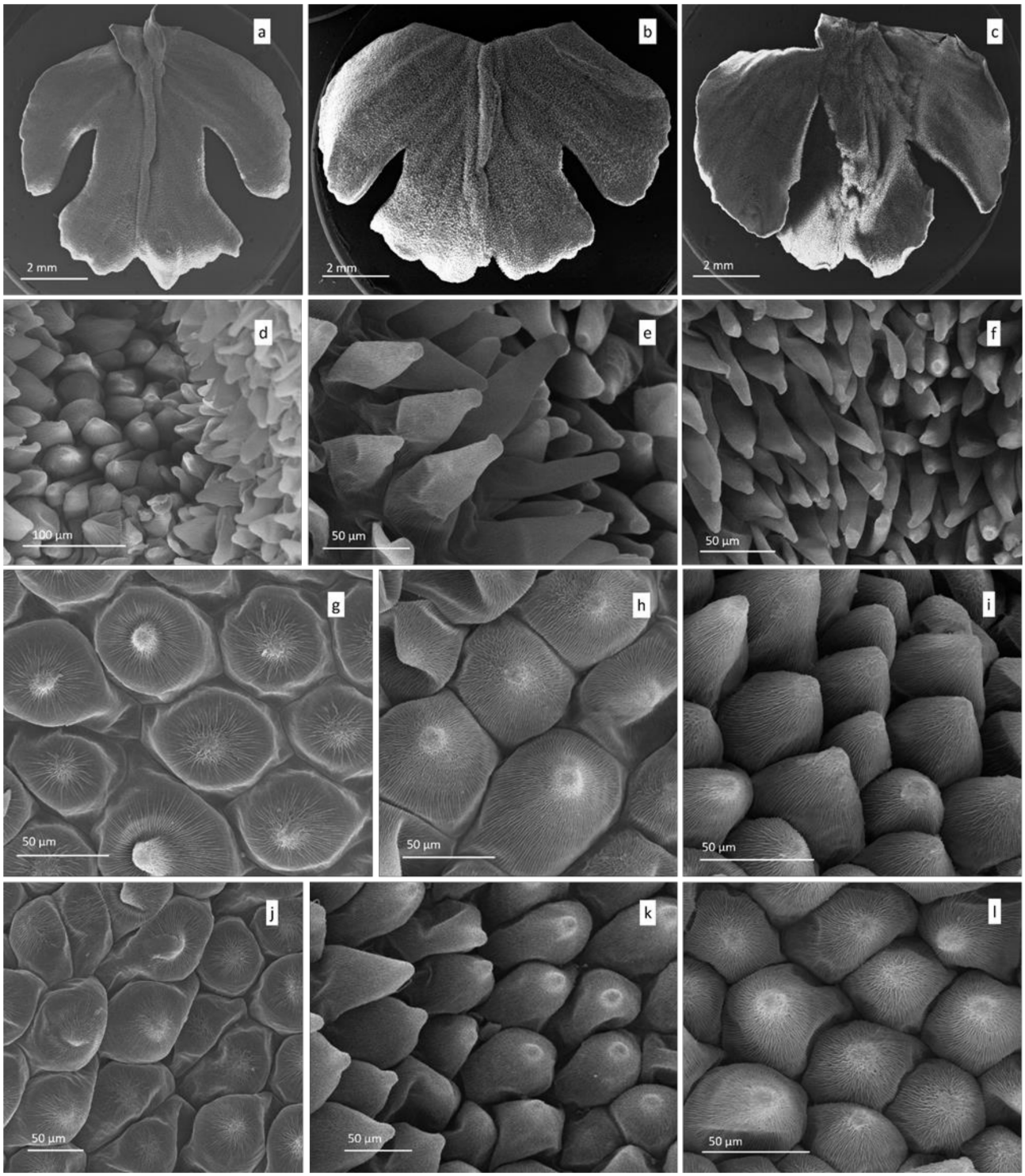

Figure 3. SEM micrographs of the labellar surfaces of the three taxa: (**a**) *O. patens*, (**b**) *O.* × *fallax*, and (**c**) *O. provincialis*. (**d**) *O. patens*: magnification of the peri-stigmatic portion of the groove, with conical/villiform papillae in the centre, and more elongated/villiform ones on the margins; (**e**) *O.* × *fallax*, peri-stigmatic portion of the groove, with conical/villiform papillae in the centre, and elongated/villiform ones on the margins. Cells are covered with sinuous/vermiform striations; (**f**) peri-stigmatic region of *O. provincialis*: villiform papillae from the groove, showing sinuous/vermiform striations; (**g**) *O. patens*: flattened papillae with radial linear/vermiform ornamentations from the labellum's arm; (**h**) *O.* × *fallax*, labellum's arm: conical papillae with radial linear/villiform striations; (**i**) *O. provincialis*: conical/villiform papillae with radial linear/vermiform ornamentations from the labellum's arm; (**j**) *O. patens*, labellum's leg: slightly conical papillae; (**k**) *O.* × *fallax*, labellum's leg: conical/villiform papillae; (**l**) conical papillae from the labellar leg of *O. provincialis*.

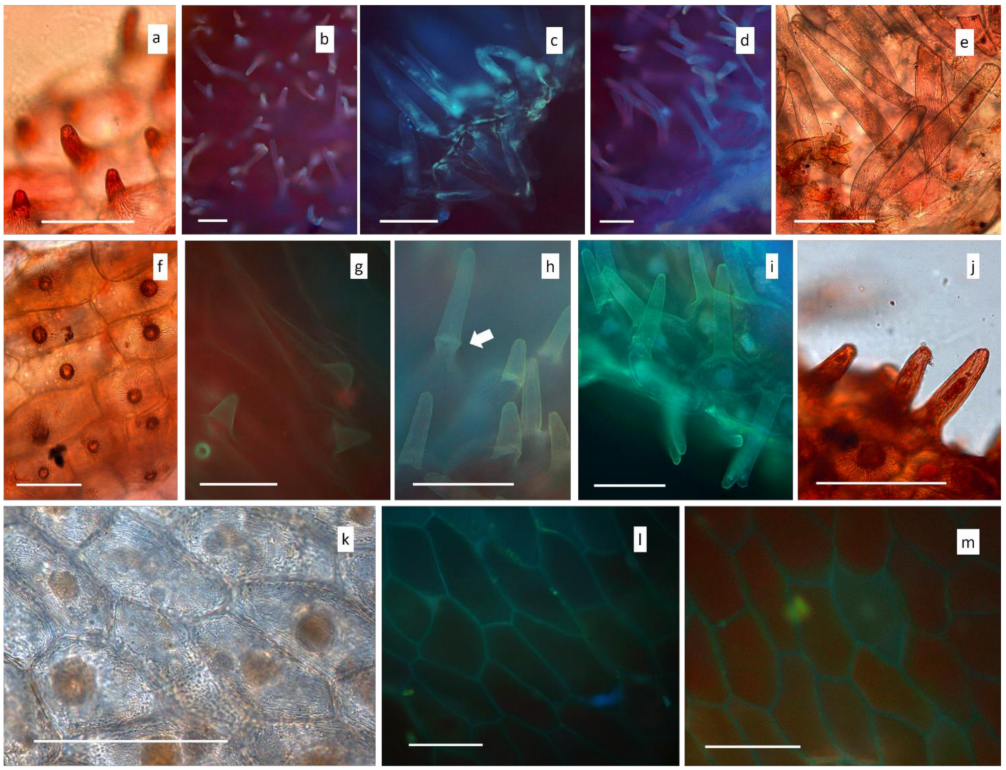

Figure 4. LM micrographs of the internal surfaces of the spur of *Orchis patens* (**a**–**e**), *O.* × *fallax* (**f**–**j**), and *O. provincialis* (**k**–**m**). Scale bars = 100 µm. (**a**) Spur entrance: small-sized conical papillae stained by Neutral Red; (**b**) distribution of medium-sized papillae in the median portion of the spur seen under UV. Polyphenolic/tannin secretions are visible within the papillae (light blue autofluorescence); anthocyanins/chlorophylls are recognizable (red autofluorescence); (**c**) polyphenolic cytoplasmatic content within elongated papillae from the protuberance near the spur apex; (**d**) distribution of elongated papillae in the spur apex; (**e**) Neutral Red positive elongated papillae from the spur apex; (**f**) small-sized conical papillae from the spur entrance, seen from above, stained by Neutral Red; (**g**) small-sized conical papillae from the entrance showing polyphenolic cytoplasmatic content; (**h**) medium-sized papillae from the median portion of the spur, showing polyphenolic secretions. Arrow indicates one of the uniseriate trichomes from this region; (**i**) light blue autofluorescence of the papillae from the protuberance near the spur apex. At the papillae bases, cytoplasmatic aggregates emitting more intense light blue signals are visible; (**j**) elongated papillae from the spur apex positive to Neutral Red; (**k**) epidermal cells showing a cytoplasmatic content weakly positive to Sudan III; (**l**) light blue autofluorescence of the cell walls in the median portion of the spur; (**m**) anthocyanin/chlorophyll/carotenoid pigments in the apical portion of the spur.

Osmophoric areas and secretory activities have been detected in the labellar surfaces (Figure 5a–f). In *O. patens* (Figure 5a) as well as both *O.* × *fallax* (Figure 5b) and *O. provincialis* (Figure 5c), both conical and villiform papillae from the labellar groove were strongly positive to Neutral Red. In this zone, residues of cytoplasmatic secreted material inside papillae were often abundant, especially in *O. provincialis*. In the three taxa, papillae from other portions of the labellum (such as torso, arms and legs) also showed Neutral Red positive cytoplasmic aggregates (Figure 5d as representative image). In *O. patens*, some conical (Figure 5e) and conical/villiform papillae of the torso emitted blue autofluorescent signals showing a polyphenolic content. Labellar papillae of *O.* × *fallax* (Figure 5f) and *O. provincialis* (not shown) presented these polyphenolic traces with higher frequency.

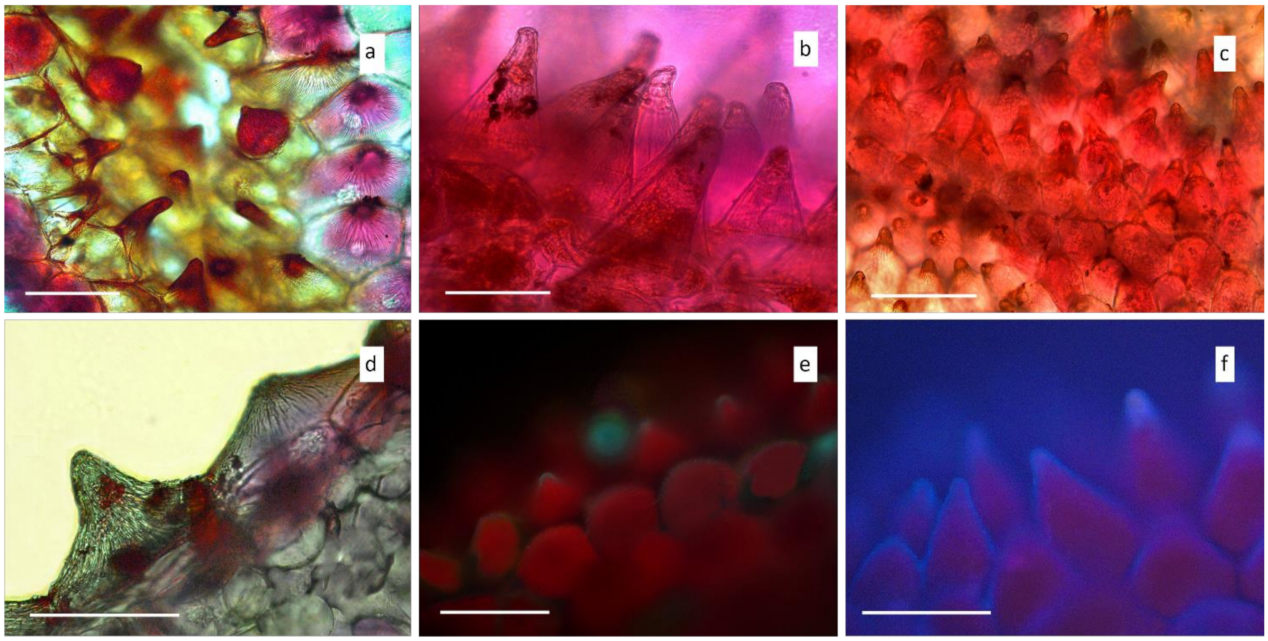

Figure 5. LM micrographs of the labellar surfaces of *Orchis patens*, *O.* × *fallax*, and *O. provincialis*. Scale bars = 100 µm. (**a**) conical and conical/villiform papillae from the centre and the margins of the labellar groove from *O. patens*. Papillae from the centre were positive to Neutral Red, while those from the lateral portions showed only the presence of rose anthocyanins; (**b**) conical/villiform papillae from the groove's margins of *O.* × *fallax* stained by Neutral Red; (**c**) conical/villiform papillae from the groove of *O. provincialis* positive to Neutral Red; (**d**) Neutral Red positive cytoplasmatic aggregates visible within conical papillae from the labellar torso of *O. patens*. Radial linear ornamentations are also recognizable on the cell surfaces; (**e**) conical papillae from the lateral portion of the torso of *O. patens* seen under UV light. Anthocyanins and polyphenols/tannins are present in the cytoplasm of some cells. Light blue signals are also present in correspondence of epicuticular waxes; (**f**) villiform papillae from the lateral portion of the torso of *O.* × *fallax*, showing light blue autofluorescent epicuticular waxes and red autofluorescent anthocyanins.

3.2. Chemical Composition of Essential Oils

Steam distillation of inflorescences of *O. patens*, *O. provincialis*, and *O.* × *fallax* yielded 83.32 mg, 37.46 mg, and 18.78 mg of yellowish oils representing 0.34%, 0.16%, and 0.13% *w*/*w* yields on dry plant materials, respectively. GC-MS and GC-FID analyses led to the identification of 31 components, listed in order of their elution and reported as percentages of the total oil. Table 1 shows the results of qualitative and quantitative analyses of essential oil. The main bulk of constituents of volatile fractions were found to be saturated hydrocarbons, accounting for 67.63%, 49.40%, and 62.59% of the total essential oils of *O. patens, O. provincialis,* and *O.* × *fallax*, respectively. This class of compounds was mainly constituted of saturated linear chain hydrocarbons in the range C_{11}–C_{27}: pentadecane (20.15% in *O. patens*), octadecane (8.97% in *O.* × *fallax*), and pentacosane (8.61% in *O. provincialis*) were the most abundant. Among saturated hydrocarbons, the odd homologs were the most representative. A series of unsaturated linear chain hydrocarbons ranging from C_{23} to C_{27} was also identified (13.74% *O. patens*, 7.33% *O. provincialis*, 3.72% *O.* × *fallax*). The double bond position in these linear isomers was determined by GC/MS after alkylthiolation reaction [47]. The most representative compounds were found to be 9-heptacosene (6.77% *O. patens*, 4.19% *O. provincialis*, 2.89% *O.* × *fallax*), 9-tricosene (1.17% *O. patens*, 0.56% *O. provincialis*, 0.82% *O.* × *fallax*), and 9-pentacosene (3.24% *O. patens*, 0.81% *O. provincialis*), followed by 7-heptacosene (1.32% *O. patens*, 0.79% *O. provincialis*) and 7-tricosene (*O. patens*, 0.98%). Other major constituents of the volatile fractions were found to be acids, accounting for 12.71% *O. patens*, 16.34% *O. provincialis*, and 16.84% *O.* × *fallax*, from which hexadecanoic acid (11.37% *O. patens*, 10.37% *O. provincialis*, 14.48% *O.* × *fallax*), dodecanoic acid (1.34% *O. patens*, 1.10% *O. provincialis*, 1.35% *O.* × *fallax*) are the most

abundant compounds, followed by nonanoic acid (2.51% *O. provincialis*, 1.0% *O.* × *fallax*), and *trans*-Cinnamic acid (2.36% *O. provincialis*). Ketones are represented by oxo-β-ionone, a β-carotene cleavage product (2.99% *O. patens*, 20.66% *O. provincialis*, 8.38 *O.* × *fallax*). Aldehydes are present in the percentage of 2.92% *O. patens*, 4.38% *O. provincialis*, and 3.83 *O.* × *fallax*, from which nonanal is the most abundant (0.81% *O. patens*, 2.46% *O. provincialis*, 2.55% *O.* × *fallax*). Other compounds belonging to this class are benzaldehyde (0.67% *O. patens*, 1.92% *O. provincialis*, 1.28% *O.* × *fallax*) and cinnamaldehyde (1.45% in *O. patens*).

Table 1. Essential oil composition (expressed as percentage) from inflorescences of the three *Orchis* taxa.

				Orchis patens	***Orchis provincialis***	***Orchis* × *fallax***	**Identification [e]**
#	**Compound [a]**	**RI [b]**	**RI [c]**	**% [d]**	**%**	**%**	
1	Benzaldehyde	953	957	0.67 ± 0.4	1.92 ± 0.2	1.28 ± 0.1	RI, NIST
2	Undecane	1100	1100	0.67 ± 0.5	0.47 ± 0.3	2.20 ± 0.1	RI, NIST
3	Nonanal	1101	1104	0.81 ± 0.9	2.46 ± 0.1	2.55 ± 0.3	RI, NIST
4	Cinnamaldehyde	1270	1271	1.45 ± 0.1	-	-	RI, NIST
5	Nonanoic acid	1276	1274	-	2.51 ± 0.2	1.00 ± 0.1	RI, NIST
6	Tetradecane	1400	1400	0.42 ± 0.2	0.74 ± 0.3	-	RI, NIST
7	*trans*-Cinnamic acid	1428	1428	-	2.36 ± 0.5	-	RI, NIST
8	Unidentified	-	1496	-	1.89 ± 0.3	4.65 ± 0.4	-
9	Pentadecane	1500	1500	20.15 ± 0.3	-	-	RI, NIST
10	Dodecanoic acid	1567	1563	1.34 ± 0.2	1.10 ± 0.1	1.35 ± 0.1	RI, NIST
11	Hexadecane	1600	1600	1.49 ± 0.7	1.57 ± 0.2	2.21 ± 0.3	RI, NIST
12	Oxo-β-ionone	1665	1665	2.99 ± 0.4	20.66 ± 0.3	8.38 ± 0.1	RI, NIST
13	Heptadecane	1700	1700	3.83 ± 0.1	4.02 ± 0.2	7.34 ± 0.2	RI, NIST
14	Octadecane	1800	1800	6.38 ± 0.1	5.63 ± 0.3	8.97 ± 0.1	RI, NIST
15	Nonadecane	1900	1900	6.06 ± 0.2	4.69 ± 01	8.49 ± 0.1	RI, NIST
16	Hexadecanoic acid	1968	1963	11.37 ± 0.1	10.37 ± 0.1	14.48 ± 0.3	RI, NIST
17	Eicosane	2000	2000	4.43 ± 0.4	4.62 ± 0.3	5.60 ± 0.1	RI, NIST
18	Heneicosane	2100	2100	4.60 ± 0.2	2.94 ± 0.2	3.25 ± 0.7	RI, NIST
19	Docosane	2200	2200	4.79 ± 0.5	4.36 ± 0.1	4.11 ± 0.2	RI, NIST
20	9-tricosene	2279	2279	1.17 ± 0.2	0.56 ± 0.4	0.82 ± 0.2	MS, RI
21	7-tricosene	2300	2290	-	0.98 ± 0.1	-	MS, RI
22	Tricosane	2300	2300	2.63 ± 0.1	2.63 ± 0.3	3.00 ± 0.3	RI, NIST
23	Tetracosane	2400	2400	1.25 ± 0.4	2.08 ± 0.2	1.49 ± 0.8	RI, NIST
24	9-pentacosene	2474	2474	3.24 ± 0.1	0.81 ± 0.5	-	MS, RI
25	7-pentacosene	2483	2489	0.74 ± 0.5	-	-	MS, RI
26	Pentacosane	2500	2500	7.16 ± 0.1	8.61 ± 0.2	7.69 ± 0.1	MS, RI
27	Hexacosane	2600	2600	0.48 ± 0.4	1.33 ± 0.1	1.17 ± 0.1	RI, NIST
28	12-heptacosene	2671	2670	0.50 ± 0.6	-	-	MS, RI
29	9-heptacosene	2676	2675	6.77 ± 0.3	4.19 ± 0.1	2.89 ± 0.1	MS, RI
30	7-heptacosene	2683	2683	1.32 ± 0.1	0.79 ± 0.4	-	MS, RI
31	Heptacosane	2700	2700	3.28 ± 0.1	5.70 ± 0.1	7.06 ± 0.3	RI, NIST
		Acids		12.71	16.34	16.84	
		Aldehydes		2.92	4.38	3.83	
		Saturated hydrocharbons		67.63	49.40	62.59	
		Unsaturated hydrocharbons		13.74	7.33	3.72	
		Ketones		2.99	20.66	8.38	
		Unidentified		-	1.89	4.65	

[a] Compounds are listed in order of elution from an Elite-5 column. [b] Retention indices according to Adams [48], unless stated otherwise. [c] Retention index (mean) determined on an Elite-5 column using a homologous series of n-hydrocarbons. [d] mean + sd of three replicates. [e] Method of identification: MS, mass spectrum; NIST, comparison with library [49]; RI, retention indices in agreement with literature values.

3.3. Fungal Metabarcoding from Roots

Illumina MiSeq sequencing was performed on roots from the three taxa (*O. provincialis*, *O.* × *fallax* and *O. patens*). After extensive quality filtering and chimera removal, reads were clustered into 870 OTUs. All the analyses reported in this study are limited to the

18 OTUs assigned to the OrM taxa Tulasnellaceae, Ceratobasidiaceae and Sebacinales (which includes Serendipitaceae and Sebacinaceae).

Most of the 18 mycorrhizal OTUs were present in all the three taxa, with the exception of five of them (Figure 6A). Only two were uniquely associated with *O. patens* (OTU524 and OTU431), belonging to Serendipitaceae and Ceratobasidiaceae respectively. Four OTUs were only shared by *O. patens* and *O.* × *fallax* (the ceratobasidioid OTU380 and the tulasnelloid OTU5) or by *O. patens* and *O. provincialis* (the serendipitoid OTU565 and the ceratobasidioid OTU 310). The most abundant OTUs (in term of number of reads) were present in the roots of the three taxa and a group of them were almost equally distributed in terms of reads frequency (Figure 6A), revealing a core of OTUs representing a common fungal symbiotic microbiota across the two parental species and their hybrid. Using a random forest approach, we classified orchid taxa based on their mycorrhizal community composition, obtaining a OOB estimate of error rate = 71.43% which reveals a strong similarity among the single orchid mycorrhizal communities. The most frequent OTUs were almost the same equally distributed across taxa (Figure 6B), as reported by the Mean Decrease Gini score, used to assess the importance of variables (in this case OTUs) in model prediction. OTU28 and OTU35 were assigned to Ceratobasidiaceae and were retrieved in all samples. Tulasnelloid fungi were strongly represented by OTU1 (*Tulasnella helicospora* cfr), the most abundant OTU; Serendipitaceae abundance was instead more variable among taxa (see Figure 6).

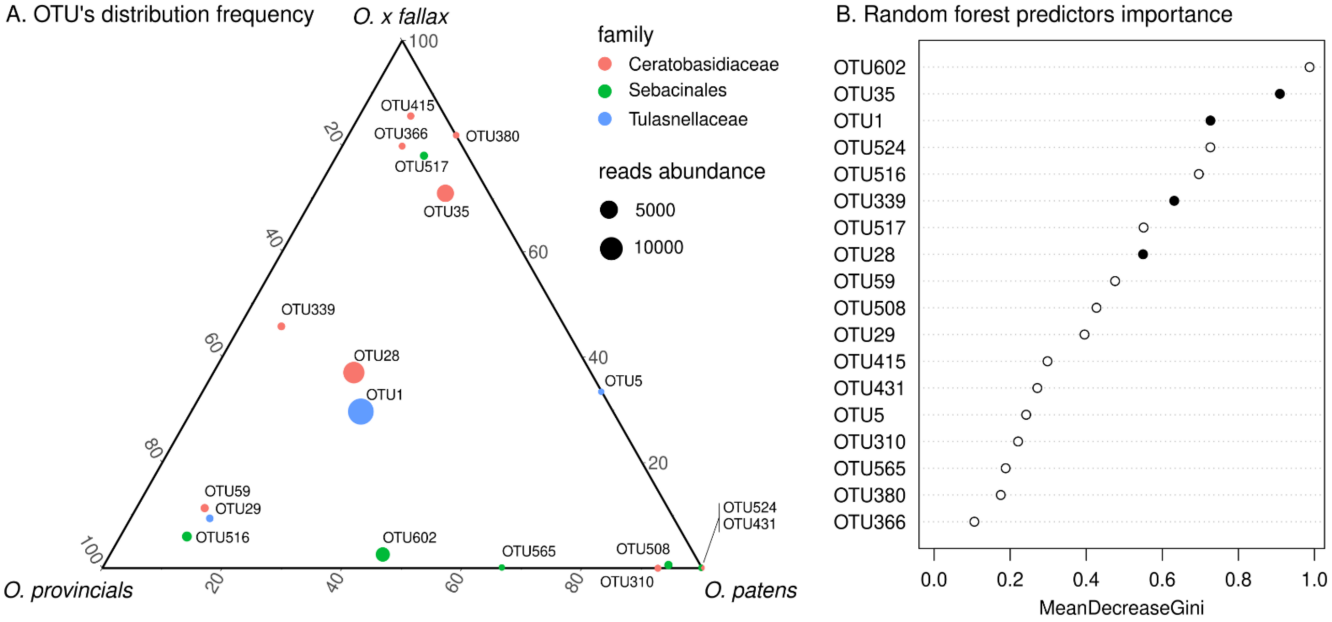

Figure 6. (**A**) Fungal OTUs are represented inside the ternary plot basing on their relative frequency (% of reads) into each plant taxon. Dot size corresponds to the OTU's reads number among all samples, and dot colors correspond to the assigned family. OTUs represented at a vertex are uniquely present in a single taxon; OTUs on an edge are shared by two taxa; OTUs inside the triangle are shared by all the taxa. (**B**) Each OTU is associated to its mean decrease in Gini score, which is a measure of variable (OTU) importance for estimating a target variable (plant taxa). The most important variables to the model are the highest. Black filled dots are the OTUs more equally shared by the three mycorrhizal communities (**A**).

4. Discussion

This study investigated floral traits and OrM fungal associations between two orchid species and their natural hybrid. The two parental species showed distinct morphological traits in their labella and spur morphology. While some hybrid traits are clearly associated with only one of the parental species, other traits appear as intermediate between the two. In other cases, the hybrid shows qualitative and quantitative traits not detected in the two parental species. Formation of novel traits in hybrids have been shown to be drivers of

ecological adaptation to new environmental conditions [71], but further work is required to see if this is the case in our study.

Orchis × *fallax* showed the presence of osmophoric papillae with polyphenolic secretions inside the spur, indicating that the character is morphologically and functionally similar and has been inherited from *O. patens*. Likewise, secretory uniseriate trichomes were detected in these two orchids. However, the abundant presence of secreted substances on the papillae surface was detected only in *O.* × *fallax*. As proposed by Kowalkowska et al. [72], the presence of polyphenolic secretions on cuticles may enhance pollinator visits through an intensification of the scent production. In *O. provincialis*, no secretory structure nor activity has been detected in the spur. As highlighted by histochemical tests, the secretory/osmophoric activity is mainly accomplished by labellar papillae. The long spur has the role of visual attraction in the deceit of pollinators by mimicking spurs or other structures typical of rewarding species [69]. Conversely, according to our results, in *O. patens* and *O.* × *fallax* floral scent could be emitted by both spur papillate epidermis and labellar papillae, especially by those located in the central labellum's groove in the case of *O. patens*. A genetic contribution from both *O. provincialis* and *O. patens* could have resulted in the intermediate length of the spur and in the single and less swollen inner protuberance present in *O.* × *fallax*. Similar protuberances have been observed also in other short-spurred orchids, for example in *Stereochilus dalatensis* (Guillaumin) Garay [73] and in another food-deceptive Mediterranean species, *Himantoglossum robertianum* (Loisel.) P. Delforge (personal observation M.B. and L.C.). These features could have the function of increasing the area of emission of volatile compounds.

As stated by Figueiredo and Pais [74], Stpiczyńska and Matusiewicz [75] and Naczk et al. [70], components being part of the floral fragrance belong to plastoglobuli which can be present in osmophores. The transportation of these products outside secretory tissues can occur through cuticular microchannels [70,76–80]. A high presence of cytoplasmatic globules and secondary metabolites has been noticed in spur papillae of *O. patens,* but especially in *O.* × *fallax*. This could be at the basis of the abundant secretion recorded by SEM. Some of the cytoplasmatic inclusions, as also confirmed by observations under UV light, could correspond to phenolic bodies already detected in species of the *Dactylorhiza maculata* complex by Naczk et al. [70]. These authors and Wiśniewska et al. [81] stated that dihydroxyphenolic globules may be involved in fragrance production, and thus we can hypothesize a similar role for cytoplasmatic inclusions that we detected in the spur and labellar papillae of *O. patens* and *O.* × *fallax.* In the hybrid, cuticular ornamentations of both spur and labellar papillae seemed to be intermediate between the two parental species. It has been proposed that cuticular striations could be involved in light reflection, acting as a visual cue for pollinators [70,82]. The hybrid showed intermediate characters also in the case of the distribution and types of labellar papillae. It has been widely reported that osmophores appear, generally, in the shape of conical papillae, and that sometimes are not discernible from other flower features [80,83,84]. By Neutral Red and autofluorescence tests, we observed that osmophoric cells and secreted substances were more frequent in the labella of *O. provincialis* and in the hybrid than in *O. patens*.

The scent of the three taxa showed dissimilarities: although the volatile spectra presented comparable percentages of compound classes (Table 1), differences were reported at the single component level. It has been proposed that even subtle fragrance variations could be determinant for floral isolation of different species growing in sympatry and sharing one or more pollinators [71,85]. While two compounds were found shared only by *O. provincialis* and *O.* × *fallax* (nonanoic acid and an unidentified compound), the hybrid did not present compounds uniquely in common with *O. patens*. On the other hand, three compounds (tetradecane, 9-pentacosene, and 7-heptacosene) were shared uniquely by *O. patens* and *O. provincialis*. Four compounds were prerogative of *O. patens* only (pentadecane, cinnamaldehyde, 7-pentacosene, and 12-pentacosene). Among these, pentadecane was recognized as the predominant compound for this species (20.15%). Two compounds were detected only in *O. provincialis* (*trans*-Cinnamic acid and 7-tricosene),

while the hybrid did not present unique molecules. Each orchid was also distinguishable for the relative abundance of single compounds. Among the various examples, one of the most notable is oxo-β-ionone, recorded as predominant in *O. provincialis* (20.66 ± 0.3 %) but present in lower amounts in *O. patens* and in intermediate quantities in *O.* × *fallax*. The occurrence in orchid scent of such cleavage product of β-carotene [86] is here reported for the first time. Results seems to suggest that unique molecules detected in the floral scent could contribute to floral isolation in the parental species. The abundant pentadecane in *O. patens* could also be involved in pollinator attraction. A further contribution by single components present in relative higher amounts in the three taxa cannot be excluded. However, the high level of hybridization and number of hybrids in the wild (Supplementary Figure S1) and a similar level of fruit set (personal observation J.C. and M.B.) suggest that pre-mating barriers are weak or absent among these taxa. It is known, indeed, that in food deceptive flowers, visual attraction is generally regarded as the primary cue to attract pollinators, while the chemical attraction plays only a secondary role in pollination [87]. While for *O. provincialis* few pollinators have been recorded such as the Anthophoridae *Eucera hungarica* and *Eucera nigrescens* or the Apidae *Bombus humilis* [88,89], no records were available for *O. patens*. The recording of the deposition of pollinia into *O. patens* stigma by *Eucera* sp. (Supplementary Figure S2) confirms that pre-mating species boundaries are not present for these species except for phenology. Indeed, the two taxa are supposed to have different flowering seasons, with *O. provincialis* flowering in late March/April and *O. patens* in late April/May [23]. However, climatic conditions more often cause a later flowering for *O. provincialis* and earlier for *O. patens* resulting in partially overlap and potential hybridization. It is important to note that fruit development in orchids is a direct result of pollination and is independent of later fertilization since pollen deposition causes ovary enlargement. [90], Consequently, estimates of fruit production can serve as indirect estimates of plant pollination success [4]. We might be careful, therefore, in considering the role of the hybrid in the distribution of the rare *O. patens*. The hybrid, indeed, always and regardless of weather conditions, overlap its flowering with both *O. provincialis* and *O. patens* (personal observation). Since there is no genetic data on the origin of *O. patens* fruit set, we cannot rule out the possibility that reproductive success was contributed by either the pollen of parental or hybrid plant and future investigations should verify this hypothesis through a manipulated cross experiment.

The analysis of putative OrM fungi by fungal metabarcoding showed that, as previously hypothesized [36], there seems to be no partitioning of OrM fungal barrier by the three taxa. Several dominant OTUs were abundant (in term of read number) in and shared by all taxa (Supplementary Figure S3). Only two OTUs were exclusive of *Orchis patens*. It is interesting to note, therefore, that contrary to what Těšitelová et al. observed in *Gymnadenia* with different ploidy levels [37], ploidy seems not to drive a shift in the OrM fungal assemblages among the sympatric taxa we investigated. Calevo et al., [36] already found that *Tulasnella helicospora*, the main OrM fungus found in *O. patens* but also *O. provincialis* and their hybrid (Figure 6; Supplementary Figure S4), is capable of inducing germination of seeds of all these taxa. The phylogenetic tree of tulasnelloid fungi (Supplementary Figure S4) revealed that also OTU5, only shared between *O. patens* and *O.* × *fallax* in fact belongs to the clade of *T. helicospora*. It is tempting to hypothesized that some "secondary" OrM fungi might play a role in restricting the distribution of *O. patens*, which is particularly rare compared to the widespread *O. provincialis*, and we cannot exclude a possible role of the two OTUs found only in *O. patens* in its distribution and persistence. The frequency of these OTUs in *O. patens* samples (75% and 50%), however, suggests that they do not play a crucial role in the ecology of this species. Comparing the OTUs sequences obtained from this study with the ones obtained in the previous work by Calevo et al. [36], we notice that not all the OTUs found by these authors were retrieved in the roots of *O. patens* (or the other orchids we investigated) (Supplementary Figures S4–S6); indeed, while the three tulasnelloid OTUs had been previously found in orchid roots (Supplementary Figure S4), only ceratobasidioid OTUs 28, 35 and 59 (the most abundant in our samples), and the

serendipitoid OTUs 524 and 517, had been previously retrieved from orchid roots, suggesting that the others OTUs found by Calevo et al. (2020) [36] are putative soil saprotrophs or plant endophytes (Supplementary Figures S5 and S6). However, in vitro experiments are required to understand their ecological roles for these orchid taxa.

5. Conclusions

Our results suggest that different floral micromorphology and chemical composition of essential oils do not differ among taxa in the hybrid zones of *Orchis patens* and *Orchis provicialis* and that OrM fungi do not vary among these taxa with different ploidy levels. These results are congruent with what was previously hypothesised by Calevo et al., [36] suggesting that OrM fungi do not limit the distribution of the endangered *O. patens*. The narrow distribution of *O. patens* seems, therefore, to be the result of abiotic factors and its lack of adaptability to environmental change. It is still not clear if the increasing abundance of *O.* × *fallax* relative to *O. patens* plays a role in limiting the distribution of *O. patens*. However, given that they share both floral traits and OrM fungi, it can potentially backcross with *O. patens* or exploit its niche and expand its range. Future studies should focus on the determination of pollinators range and observation of their behaviour on the parental species and their hybrid on fitness components among these hybridizing Mediterranean orchids to test how hybrids influence the distribution of their parental taxa (and if they constitute a threat to their long-term survival).

Supplementary Materials: The following are available online at https://www.mdpi.com/article/10.3390/d13110550/s1. Figure S1: Stacked column chart of the percentage of hybrid plants within populations in Liguria, Italy. Populations are listed geographically from East to West. Figure S2: *Eucera* sp. depositing pollinia on *Orchis patens* stigma. Figure S3: Relative abundance in term of read number of the main OTUs found in *Orchis provincialis*, *Orchis* × *fallax* and *Orchis patens*. Figure S4: Maximum likelihood tree obtained from the ITS2 sequence alignment of tulasnelloid fungi. *Multicalvula vernalis* was used as outgroup. Bootstrap support values above 70% (1000 maximum likelihood replicates) are reported. The same database used in Calevo et al. (2020) was here adopted. OTUs found in this study are indicated in bald green, soil samples and root samples from Calevo et al. (2020) are in red and blue, respectively. Figure S5: Maximum likelihood tree obtained from the ITS2 sequence alignment of ceratobasidioid fungi. *Tricholoma portentosum* and *Laccaria bicolor* were used as outgroup taxa. Bootstrap support values above 70% (1000 maximum likelihood replicates) are reported. The same database used in Calevo et al. (2020) was here adopted. OTUs found in this study are indicated in bald green, soil samples and root samples from Calevo et al. (2020) are in red and blue, respectively. Figure S6: Maximum likelihood tree obtained from the ITS2 sequence alignment of fungi assigned to Sebacinales. Paulisebacina allantoidea was used as an outgroup taxon. Bootstrap support values above 70% (1000 maximum likelihood replicates) are reported. The same database used in Calevo et al. (2020) was here adopted. OTUs found in this study are indicated in bald green, soil samples and root samples from Calevo et al. (2020) are in red and blue, respectively.

Author Contributions: Conceptualization, J.C., M.B.; methodology, J.C., M.B., M.A., S.V. and F.S.R.d.C.; formal analysis, J.C., M.B., M.A. and F.S.R.d.C.; investigation, J.C., M.B., M.A. and F.S.R.d.C.; resources, J.C., A.G., L.C., M.G. and F.S.R.d.C.; data curation, J.C., M.B., M.A. and F.S.R.d.C.; writing—original draft preparation, J.C., M.B., M.A., K.J.D. and F.S.R.d.C.; writing—review and editing. All authors have read and agreed to the published version of the manuscript.

Funding: This research received no external funding.

Institutional Review Board Statement: Not applicable.

Data Availability Statement: Representative ITS-rDNA sequences are deposited in GenBank under the following string of accession numbers: OK335158-OK335175.

Acknowledgments: Authors are very thankful to Laura Negretti (University of Genova) for SEM assistance and Arianna Cassetti (CREA-OF) for microscopy technical support.

Conflicts of Interest: The authors declare no conflict of interest.

References

1. Anderson, E. *Introgressive Hybridization*; Wiley: New York, NY, USA, 1949.
2. Stebbins, G.L. The role of hybridization in evolution. *Proc. Am. Philos. Soc.* **1959**, *103*, 231–251.
3. Soltis, D.E.; Soltis, P.S. Polyploidy: Recurrent formation and genome evolution. *Trends Ecol. Evol.* **1999**, *14*, 348–352. [CrossRef]
4. Cozzolino, S.; Nardella, A.; Impagliazzo, S.; Widmer, A.; Lexer, C. Hybridization and conservation of Mediterranean orchids: Should we protect the orchid hybrids or the orchid hybrid zones? *Biol. Conserv.* **2006**, *129*, 14–23. [CrossRef]
5. Qiu, T.; Liu, Z.; Liu, B. The effects of hybridization and genome doubling in plant evolution via allopolyploidy. *Mol. Biol. Rep.* **2020**, *47*, 5549–5558. [CrossRef]
6. Kim, J.K.; Bae, S.E.; Lee, S.J.; Yoon, M.G. New insight into hybridization and unidirectional introgression between *Ammodytes japonicus* and *Ammodytes Heian* (Trachiniformes, Ammodytidae). *PLoS ONE* **2017**, *12*, e0178001. [CrossRef] [PubMed]
7. Todesco, M.; Pascual, M.A.; Owens, G.L.; Ostevik, K.L.; Moyers, B.T.; Hübner, S.; Heredia, S.M.; Hahn, M.A.; Caseys, C.; Bock, D.G.; et al. Hybridization and extinction. *Evol. Appl.* **2016**, *9*, 892–908. [CrossRef] [PubMed]
8. Ellstrand, N.C.; Schierenbeck, K.A. Hybridization as a stimulus for the evolution of invasiveness in plants. *Proc. Natl. Acad. Sci. USA* **2000**, *97*, 7043–7050. [CrossRef] [PubMed]
9. Ferdy, J.B.; Austerlitz, F. Extinction and introgression in a community of partially cross-fertile plant species. *Am. Nat.* **2002**, *160*, 74–86. [CrossRef]
10. Allendorf, F.W.; Leary, R.F.; Spruell, P.; Wenburg, J.K. The problems with hybrids: Setting conservation guidelines. *Trends Ecol. Evol.* **2001**, *16*, 613–622. [CrossRef]
11. Arnold, M.L. *Natural Hybridization and Evolution*; Oxford University Press: New York, NY, USA, 1997.
12. Bersweden, L.; Viruel, J.; Schatz, B.; Harland, J.; Gargiulo, R.; Cowan, R.S.; Calevo, J.; Juan, A.; Clarkson, J.J.; Leitch, A.R.; et al. Microsatellites and petal morphology reveal new patterns of admixture in *Orchis* hybrid zones. *Am. J. Bot.* **2021**, *108*, 1388–1404. [CrossRef] [PubMed]
13. Coyne, J.A.; Orr, H.A. *Speciation*; Sinauer: Sunderland, MA, USA, 2004.
14. Mota, M.R.; Pinheiro, F.; Leal, B.S.S.; Wendt, T.; Palma-Silva, C. The role of hybridization and introgression in maintaining species integrity and cohesion in naturally isolated inselberg bromeliad populations. *Plant Biol.* **2019**, *21*, 122–132. [CrossRef]
15. Abbott, R.J.; Albach, D.; Ansell, S.; Arntzen, J.W.; Baird, S.J.E.; Bierne, N.; Boughman, J.; Brelsford, A.; Buerkle, C.A.; Buggs, R.; et al. Hybridization and speciation. *J. Evol. Biol.* **2013**, *26*, 229–246. [CrossRef] [PubMed]
16. Yan, L.J.; Burgess, K.S.; Zheng, W.; Tao, Z.B.; Li, D.Z.; Gao, L.M. Incomplete reproductive isolation between *Rhododendron* taxa enables hybrid formation and persistence. *J. Integr. Plant Biol.* **2019**, *61*, 433–448. [CrossRef] [PubMed]
17. Christenhusz, M.J.M.; Byng, J.W. The number of known plants species in the world and its annual increase. *Phytotaxa* **2016**, *261*, 201–217. [CrossRef]
18. Willing, B.; Willing, E. Bibliographie über die Orchideen Europas und der Mittelmeerländer. *Englera* **1985**, *5*, 1–280. [CrossRef]
19. Scopece, G.; Musacchio, A.; Widmer, A.; Cozzolino, S. Patterns of reproductive isolation in Mediterranean deceptive orchids. *Evolution* **2007**, *61*, 2623–2642. [CrossRef]
20. Scopece, G.; Widmer, A.; Cozzolino, S. Evolution of postzygotic reproductive isolation in a guild of deceptive orchids. *Am. Nat.* **2008**, *171*, 315–326. [CrossRef] [PubMed]
21. Pellegrino, G.; Bellusci, F.; Musacchio, A. Genetic integrity of sympatric hybridising plant species: The case of *Orchis italica* and *O. anthropophora*. *Plant Biol.* **2009**, *11*, 434–441. [CrossRef]
22. Cozzolino, S.; Widmer, A. Orchid diversity: An evolutionary consequence of deception? *Trends Ecol. Evol.* **2005**, *20*, 487–494. [CrossRef]
23. Kretzschmar, H.; Eccarius, W.; Dietrich, H. *The Orchid Genera Anacamptis, Orchis, Neotinea*; Echinomedia Verlag: Bürgel, Germany, 2007.
24. Jacquemyn, H.; Brys, R.; Honnay, O.; Roldán-Ruiz, I.; Lievens, B.; Wiegand, T. Nonrandom spatial structuring of orchids in a hybrid zone of three *Orchis* species. *New Phytol.* **2012**, *193*, 454–464. [CrossRef]
25. Joffard, N.; Massol, F.; Grenié, M.; Montgelard, C.; Schatz, B. Effect of pollination strategy, phylogeny and distribution on pollination niches of Euro-Mediterranean orchids. *J. Ecol.* **2019**, *107*, 478–490. [CrossRef]
26. Schatz, B.; Genoud, D.; Claessens, J.; Kleynen, J. Orchid–pollinator network in Euro-Mediterranean region: What we know, what we think we know, and what remains to be done. *Acta Oecol.* **2020**, *107*, 103605. [CrossRef]
27. Moccia, M.D.; Widmer, A.; Cozzolino, S. The strength of reproductive isolation in two hybridizing food-deceptive orchid species. *Mol. Ecol.* **2007**, *16*, 2855–2866. [CrossRef]
28. Cozzolino, S.; Scopece, G. Specificity in pollination and consequences for postmating reproductive isolation in deceptive Mediterranean orchids. *Philos. Trans. R. Soc. Lond. B Biol. Sci.* **2008**, *363*, 3037–3046. [CrossRef]
29. Stebbins, G.L. *Chromosomal Evolution in Higher Plants*; Edward Arnol: London, UK, 1971.
30. De hert, K.; Jacquemyn, H.; Van Glabeke, S.; Roldán-Ruiz, I.; Vandepitte, K.; Leus, L.; Honnay, O. Reproductive isolation and hybridization in sympatric populations of three *Dactylorhiza* species (Orchidaceae) with different ploidy levels. *Ann. Bot.* **2012**, *109*, 709–720. [CrossRef] [PubMed]
31. Rasmussen, H.N. *Terrestrial Orchids from Seed to Mycotrophic Plant*; Cambridge University Press: Cambridge, UK, 1995.
32. Smith, S.E.; Read, D.J. *Mycorrhizal Symbiosis*, 2nd ed.; Academic Press: Cambridge, UK, 2008.
33. Hollick, P.S.; Taylor, R.J.; McComb, J.A.; Dixon, K.W. If orchid mycorrhizal fungi are so specific, how do natural hybrids cope? *Selbyana* **2005**, *26*, 159–170.

34. Jacquemyn, H.; Merckx, V.; Brys, R.; Tyteca, D.; Cammue, B.P.A.; Honnay, O.; Lievens, B. Analysis of network architecture reveals phylogenetic constraints on mycorrhizal specificity in the genus Orchis (*Orchidaceae*). *New Phytol.* **2011**, *192*, 518–528. [CrossRef] [PubMed]
35. Shefferson, R.P.; Bunch, W.; Cowden, C.C.; Lee, Y.I.; Kartzinel, T.R.; Yukawa, T.; Downing, J.; Jiang, H. Does evolutionary history determine specificity in broad ecological interactions? *J. Ecol.* **2019**, *107*, 1582–1593. [CrossRef]
36. Calevo, J.; Voyron, S.; Ercole, E.; Girlanda, M. Is the Distribution of Two Rare *Orchis* Sister Species Limited by Their Main Mycobiont? *Diversity* **2020**, *12*, 262. [CrossRef]
37. Těšitelová, T.; Jersáková, J.; Roy, M.; Kubátová, B.; Těšitel, J.; Urfus, T.; Trávníček, P.; Suda, J. Ploidy-specific symbiotic interactions: Divergence of mycorrhizal fungi between cytotypes of the *Gymnadenia conopsea* group (Orchidaceae). *New Phytol.* **2013**, *199*, 1022–1033. [CrossRef]
38. Calevo, J.; Gargiulo, R.; Bersweden, L.; Viruel, J.; González-Montelongo, C.; Rhebbas, K.; Boutabia, L.; Fay, M.F. Molecular evidence of species- and subspecies-level distinctions in the rare *Orchis patens s.l.* and implications for conservation. *Biodivers. Conserv.* **2021**, *30*, 1293–1314. [CrossRef]
39. Pellegrino, G.; Cozzolino, S.; D'Emerico, S.; Grunanger, P. The taxonomic position of the controversial taxon *Orchis clandestina* (Orchidaceae): Karyomorphological and molecular analyses. *Bot. Helv.* **2000**, *110*, 101–107.
40. Talamond, P.; Verdeil, J.L.; Conéjéro, G. Secondary metabolite localization by autofluorescence in living plant cells. *Molecules* **2015**, *20*, 5024–5037. [CrossRef] [PubMed]
41. Stern, W.L.; Curry, K.J.; Whitten, W.M. Staining Fragrance Glands in Orchid Flowers. *Bull. Torrey Bot. Club* **1986**, *113*, 288–297. [CrossRef]
42. Chieco, C.; Rotondi, A.; Morrone, L.; Rapparini, F.; Baraldi, R. An ethanol-based fixation method for anatomical and micromorphological characterization of leaves of various tree species. *Biotech. Histochem.* **2013**, *88*, 109–119. [CrossRef]
43. Bateman, R.M.; Molnár, V.A.; Sramkó, G. In situ morphometric survey elucidates the evolutionary systematics of the Eurasian *Himantoglossum* clade (Orchidaceae: Orchidinae). *PeerJ* **2017**, *5*, e2893. [CrossRef] [PubMed]
44. Akbulut, M.K.; Şenel, G.; Şeker, Ş.S. Comparison of labellum and spur papillae in *Dactylorhiza* (Orchidaceae) from Anatolia. *Braz. J. Bot.* **2020**, *43*, 367–377. [CrossRef]
45. Robustelli della Cuna, F.S.; Calevo, J.; Bari, E.; Giovannini, A.; Boselli, C.; Tava, A. Characterization and Antioxidant Activity of Essential Oil of Four Sympatric Orchid Species. *Molecules* **2019**, *24*, 3878. [CrossRef]
46. Robustelli della Cuna, F.S.; Giovannini, A.; Braglia, L.; Sottani, C.; Preda, S. Chemical Composition of the Essential Oil from Leaves and Flowers of *Passiflora sexocellata* and *Passiflora trifasciata* (Passifloraceae). *Nat. Prod. Commun.* **2021**, *16*, 1–7. [CrossRef]
47. Carlson, D.A.; Roan, C.S.; Yost, R.A.; Hector, J. Dimethyl disulphide derivatives of long chain alkenes, alkadienes and alkatrienes for gas chromatography/mass spectrometry. *Anal. Chem.* **1989**, *61*, 1564–1571. [CrossRef]
48. Adams, R. *Identification of Essential Oil Components by Gas Chromatography/Mass Spectrometry*, 4th ed.; Allured Publishing Corporation: Carol Stream, IL, USA, 2007.
49. Joulain, D.; Konig, W.A. (Eds.) The atlas of spectral data of sesquiterpene hydrocarbons. In *NIST/EPA/NIH Mass Spectral Database*; Version 2.1 Perkin-Elmer Instrument LLC, Copyright ©. 2000; E. B. Verlag: Hamburg, Germany, 1998.
50. Taylor, D.L.; McCormick, M.K. Internal transcribed spacer primers and sequences for improved characterization of basidiomycetous orchid mycorrhizas. *New Phytol.* **2008**, *177*, 1020–1033. [CrossRef]
51. White, T.J.; Bruns, T.; Lee, S.; Taylor, J.W. Amplification and direct sequencing of fungal ribosomal RNA genes for phylogenetics. In *PCR Protocols: A Guide to Methods and Applications*; Innis, M.A., Gelfand, D.H., Sninsky, J.J., White, T.J., Eds.; Academic Press: New York, NY, USA, 1990; pp. 315–322.
52. Voyron, S.; Ercole, E.; Ghignone, S.; Perotto, S.; Girlanda, M. Fine-scale spatial distribution of orchid mycorrhizal fungi in the soil of host-rich grasslands. *New Phytol.* **2017**, *213*, 1428–1439. [CrossRef]
53. Zang, J.; Kobert, K.; Flouri, T.; Stamatakis, A. PEAR: A fast and accurate Illumina Paired-End reAd mergeR. *Bioinformatics* **2014**, *30*, 614–620. [CrossRef]
54. Caporaso, J.G.; Kuczynski, J.; Stombaugh, J.; Bittinger, K.; Bushman, F.D.; Costello, E.K.; Fierer, N.; Pena, A.G.; Goodrich, J.K.; Gordon, J.I.; et al. QIIME allows analysis of high-throughput community sequencing data. *Nat. Methods* **2010**, *7*, 335–336. [CrossRef]
55. Edgar, R.C. Search and clustering orders of magnitude faster than BLAST. *Bioinformatics* **2010**, *26*, 2460–2461. [CrossRef]
56. Abarenkov, K.; Nilsson, R.H.; Larsson, K.H.; Alexander, I.J.; Eberhardt, U.; Erland, S.; Hoiland, K.; Kjoller, R.; Larsson, E.; Pennanen, T.; et al. The UNITE database for molecular identification of fungi—Recent updates and future perspectives. *New Phytol.* **2010**, *186*, 281–285. [CrossRef] [PubMed]
57. Koljalg, U.; Nilsson, R.H.; Abarenkov, K.; Tedersoo, L.; Taylor, A.F.S.; Bahram, M.; Bates, S.T.; Bruns, T.D.; Bengtsson-Palme, J.; Callaghan, T.M.; et al. Towards a unified paradigm for sequence-based identification of fungi. *Mol. Ecol.* **2013**, *22*, 5271–5277. [CrossRef]
58. Altschul, S.F.; Gish, W.; Miller, W.; Myers, E.W.; Lipman, D.J. Basic local alignment search tool. *J. Mol. Biol.* **1990**, *215*, 403–410. [CrossRef]
59. Edgar, R.C. MUSCLE: Multiple sequence alignment with high accuracy and high throughput. *Nucleic Acids Res.* **2004**, *32*, 1792–1797. [CrossRef]

60. Kumar, S.; Stecher, G.; Tamura, K. MEGA7: Molecular evolutionary genetics analysis version 7.0 for bigger datasets. *Mol. Biol. Evol.* **2016**, *33*, 1870–1874. [CrossRef] [PubMed]
61. Stamatakis, A. RAxML version 8: A tool for phylogenetic analysis and post-analysis of large phylogenies. *Bioinformatics* **2014**, *3030*, 1312–1313. [CrossRef]
62. Felsenstein, J. Confidence limits on phylogenies: An approach using the bootstrap. *Evolution* **1985**, *39*, 783–791. [CrossRef]
63. Miller, M.A.; Pfeiffer, W.; Schwartz, T. Creating the CIPRES Science Gateway for inference of large phylogenetic trees. In Proceedings of the Gateway Computing Environments Workshop (GCE), New Orleans, LA, USA, 14 November 2010; pp. 1–8.
64. R Core Team. *R: A Language and Environment for Statistical Computing*; R Foundation for Statistical Computing: Vienna, Austria, 2021. Available online: https://www.R-project.org/ (accessed on 3 September 2021).
65. RStudio Team. *RStudio: Integrated Development Environment for R*; RStudio, PBC: Boston, MA, USA, 2021. Available online: http://www.rstudio.com/ (accessed on 3 September 2021).
66. Hamilton, N.E.; Ferry, M. ggtern: Ternary Diagrams Using ggplot2. *J. Stat. Softw.* **2018**, *87*, 1–17. [CrossRef]
67. Ho, T.K. Random decision forests. In Proceedings of the 3rd International Conference on Document Analysis and Recognition, Montreal, QC, Canada, 14–16 August 1995; Volume 1, pp. 278–282. [CrossRef]
68. Liaw, A.; Wiener, M. Classification and regression by randomForest. *R News* **2002**, *2*, 18–22.
69. Bell, A.; Roberts, D.; Hawkins, J.; Rudall, P.; Box, M.; Bateman, R. Comparative micromorphology of nectariferous and nectarless labellar spurs in selected clades of subtribe Orchidinae (Orchidaceae). *Bot. J. Linn. Soc.* **2009**, *160*, 369–387. [CrossRef]
70. Naczk, A.M.; Kowalkowska, A.K.; Wiśniewska, N.P.; Haliński, L.P.; Kapusta, M.; Czerwicka, M. Floral anatomy, ultrastructure and chemical analysis in *Dactylorhiza incarnata/maculate* complex (Orchidaceae). *Bot. J. Linn. Soc.* **2018**, *187*, 512–536. [CrossRef]
71. Rieseberg, L.H.; Raymond, O.; Rosenthal, D.M.; Lai, Z.; Livingstone, K.; Nakazato, T.; Durphy, J.L.; Schwarzbach, A.E.; Donovan, L.A.; Lexer, C. Major ecological transitions in wild sunflowers facilitated by hybridization. *Science* **2003**, *301*, 1211–1216. [CrossRef]
72. Kowalkowska, A.K.; Pawłowicz, M.; Guzanek, P.; Krawczyńska, A.T. Floral nectary and osmophore of *Epipactis helleborine* (L.) Crantz (Orchidaceae). *Protoplasma* **2018**, *255*, 1811–1825. [CrossRef] [PubMed]
73. Stpiczyńska, M.; Davies, K.; Kamińska, M. Comparative anatomy of the nectar spur in selected species of Aeridinae (Orchidaceae). *Ann. Bot.* **2010**, *107*, 327–345. [CrossRef] [PubMed]
74. Figueiredo, A.C.S.; Pais, M.S. Ultrastructural aspects of the nectary spur of *Limodorum abortivum* (L.) Sw. (Orchidaceae). *Ann. Bot.* **1992**, *70*, 325–331. [CrossRef]
75. Stpiczyńska, M.; Matusiewicz, J. Anatomy and ultrastructure of spur nectary of *Gymnadenia conopsea* L. (Orchidaceae). *Acta Soc. Bot. Pol.* **2001**, *70*, 267–272. [CrossRef]
76. Pridgeon, A.M.; Stern, W.L. Osmophores of *Scaphosepalum* (Orchidaceae). *Bot. Gaz.* **1985**, *146*, 115–123. [CrossRef]
77. Stern, W.L.; Curry, K.J.; Pridgeon, A.M. Osmophores of *Stanhopea* (Orchidaceae). *Am. J. Bot.* **1987**, *74*, 1323–1331. [CrossRef]
78. Pais, M.S.S.; Figueiredo, A.C.S. Floral nectaries from *Limodorum abortivum* (L.) Sw. and *Epipactis atropurpurea* Rafin (Orchidaceae): Ultrastructural changes in plastids during the secretory process. *Apidologie* **1994**, *25*, 615–626. [CrossRef]
79. Stpiczyńska, M. The structure of nectary of *Platanthera bifolia* L. (Orchidaceae). *Acta Soc. Bot. Pol.* **1997**, *62*, 5–9. [CrossRef]
80. Kowalkowska, A.K.; Margońska, H.B.; Kozieradzka-Kiszkurno, M.; Bohdanowicz, J. Studies on the ultrastructure of a three-spurred *fumeauxiana* form of *Anacamptis pyramidalis*. *Plant Syst. Evol.* **2012**, *298*, 1025–1035. [CrossRef]
81. Wiśniewska, N.; Kowalkowska, A.K.; Kozieradzka-Kiszkurno, M.; Krawczyńska, A.T.; Bohdanowicz, J. Floral features of two species of *Bulbophyllum* section Lepidorhiza Schltr.: B. levanae Ames and B. nymphopolitanum Kraenzl. (Bulbophyllinae Schltr. Orchidaceae). *Protoplasma* **2018**, *255*, 485–499. [CrossRef]
82. Davies, K.L.; Stpiczynska, M.; Turner, M.P. A rudimentary labellar speculum in *Cymbidium lowianum* (Rchb.f.) Rchb.f. and *Cymbidium devonianum* Paxton (Orchidaceae). *Ann. Bot.* **2006**, *97*, 975–984. [CrossRef] [PubMed]
83. Stpiczyńska, M. Osmophores of the fragrant orchid *Gymnadenia conopsea* L. (Orchidaceae). *Acta Soc. Bot. Pol.* **2001**, *70*, 91–96. [CrossRef]
84. Teixeira Sde, P.; Borba, E.L.; Semir, J. Lip anatomy and its implications for the pollination mechanisms of *Bulbophyllum* species (Orchidaceae). *Ann. Bot.* **2004**, *93*, 499–505. [CrossRef] [PubMed]
85. Waelti, M.O.; Muhlemann, K.; Widmer, A.; Schiestl, F.P. Floral odour and reproductive isolation in two species of *Silene*. *J. Evol. Biol.* **2008**, *21*, 111–121. [CrossRef] [PubMed]
86. Alija, A.J.; Bresgen, N.; Sommerburg, O.; Langhans, C.D.; Siems, W.; Eckl, P.M. Cyto- and genotoxic potential of beta-carotene and cleavage products under oxidative stress. *Biofactors* **2005**, *24*, 159–163. [CrossRef] [PubMed]
87. Dafni, A. Floral mimicry-mutualism and unidirectional exploitation of insects by plants. In *The Plant Surface and Insects*; Southwood, T.R.E., Juniper, B.E., Eds.; Edward Arnold: London, UK, 1986; pp. 81–90.
88. G.I.R.O.S.-Gruppo Italiano per la Ricerca Sulle Orchidee Spontanee • Leggi Argomento-Generi: Anacamptis, Neotinea, Orchis (giros.it). Available online: http://www.giros.it/forum/viewtopic.php?f=131&t=1498&sid=f261715f17a25c493beedc63a8b740fb (accessed on 1 October 2021).
89. Cozzolino, S.; Schiestl, F.P.; Müller, A.; De Castro, O.; Nardella, A.M.; Widmer, A. Evidence for pollinator sharing in Mediterranean nectar-mimic orchids: Absence of premating barriers? *Proc. Biol. Sci.* **2005**, *272*, 1271–1278. [CrossRef] [PubMed]
90. O'Neill, S.D.; Nadeau, J.A.; Zhang, X.S.; Bui, A.Q.; Halevy, A.H. Interorgan regulation of ethylene biosynthetic genes by pollination. *Plant Cell* **1993**, *5*, 419–432. [PubMed]